

One Code to Fit Them All: Forward-Folding AGN Spectra Over 11 Energy Decades with Gammapy

Mireia Nievas Rosillo,^{a,b,*} Fabio Acero,^{c,d} Jorge Otero Santos,^{e,f} Daniel Morcuende,^{e,g} Regis Terrier^h and Lea Alina Heckmann^h

^a*Instituto de Astrofísica de Canarias (IAC), C/ Vía Láctea s/n, 38205 La Laguna, Spain*

^b*Universidad de La Laguna (ULL), Avda. Astrofísico Francisco Sánchez s/n, 38206 La Laguna, Spain*

^c*FSLAC IRL 2009, CNRS/IAC, C/ Vía Láctea s/n, 38205 La Laguna, Tenerife, Spain*

^d*AIM, CEA, CNRS, Université Paris–Saclay, Université de Paris, 91191 Gif-sur-Yvette, France*

^e*Instituto de Astrofísica de Andalucía (IAA-CSIC), Glorieta de la Astronomía s/n, 18008 Granada, Spain*

^f*Istituto Nazionale di Fisica Nucleare, Sezione di Padova, 35131 Padova, Italy*

^g*Cherenkov Telescope Array Observatory (CTAO), Platanenallee 6, 15738 Zeuthen, Germany*

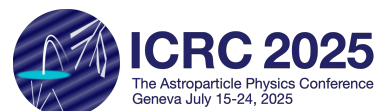
^h*APC, Université de Paris, CNRS, CEA, Observatoire de Paris, 10 rue Alice Domon et Léonie Duquet, 75013 Paris, France*

E-mail: mnievas@iac.es

Most modern studies of Active Galactic Nuclei (AGN) rely on broadband spectral analyses to constrain the plethora of particle acceleration and emission processes. Traditional analysis methods are often hindered by the use of proprietary tools tailored for each participating instrument, making it challenging to integrate multi-wavelength data in a consistent, reproducible, and statistically correct way.

In this work, we present a unified framework using the open-source tool *gammapy* to perform a forward-folding spectral analysis of AGN data from the optical to gamma-rays (over 11 decades in energy), enabling the full incorporation of instrument response functions and astrophysical backgrounds, while reducing biases associated with the traditional flux point analysis. It also offers a flexible and compact data format to store and distribute the data and telescope information. We demonstrate its capabilities with data from the quasars OP 313 and 4C +27.50, which underwent flaring activity during 2024. Our analysis includes optical data from the Liverpool Telescope, UV data from *Swift*-UVOT, X-ray data from *Swift*-XRT and NuSTAR, and gamma-ray data from *Fermi*-LAT. We validate the analysis against native tools for each instrument, and discuss the prospects for future multi-wavelength and time-domain astrophysical studies of AGN.

39th International Cosmic Ray Conference (ICRC2025)
15–24 July 2025
Geneva, Switzerland



*Speaker

Active Galactic Nuclei (AGN), in particular those with jetted emission aligned with the line of sight, or blazars, are among the most luminous long-lived non-thermal sources in the universe. They radiate across the electromagnetic spectrum, from radio to TeV γ rays. Broadband multi-wavelength studies of AGN flares are key to understanding the physical mechanisms behind the emission, locating the emission sites, and ultimately understanding how particles are accelerated. However, combining data from optical, UV, X-ray, and gamma-ray data from a heterogeneous set of both ground-based and space-borne instrumentation poses multiple challenges and often oversimplified stitching together flux points that inherently assume incorrect Gaussian statistics and ignore correlations.

In this contribution, we introduce an end-to-end workflow based on the open-source analysis package `gammapy` to perform forward-folding-based spectral analysis across eleven decades in energy. By ingesting raw count spectra and appropriate instrument response functions (IRFs) for each instrument, our approach has a more appropriate assumption on the underlying statistics for each instrument, naturally incorporating correlations within each band, taking into account non-detection, and allowing us to easily test systematic uncertainties. All while unifying all wavebands under a single likelihood framework and fitting routine. We demonstrate the utility of this method on multi-wavelength observations of two flaring quasars, highlighting its accuracy, reproducibility, and potential for large-scale AGN population studies.

1. Dataset Construction

The core ingredient of a `gammapy` analysis is the concept of `dataset`. Datasets in `gammapy` can be of different types, depending on the nature of the instrument and its data products:

1.1 3D Spatial–Spectral Datasets (*Fermi-LAT*)

For *Fermi-LAT* we build a `MapDataset` or 3D dataset, comprising

- A counts cube in RA–Dec–energy dimensions, acquired over a fixed integration time window.
- An exposure cube and point-spread-function cube derived from the `gtl1tcube` and `gtexpcube2` tools, whose spatial and energy axes are aligned with those from the counts cube for simplicity.
- A PSF kernel map (spatial redistribution of events)
- An energy-dispersion kernel map (energy-redistribution of events, linking true and reconstructed energies)
- A background model using the official Galactic interstellar emission and isotropic templates plus a set of point and extended source models inside a given region of interest, which may contaminate the position of our target blazar.

This 3D dataset enables simultaneous spatial and spectral fitting of the AGN and nearby sources, fully accounting for PSF broadening and energy dispersion in the likelihood. For blazars and point-like sources, however, usually the spatial component is frozen to that from a catalog (most always for blazars a point-like source) and only the spectral components are fit to the data.

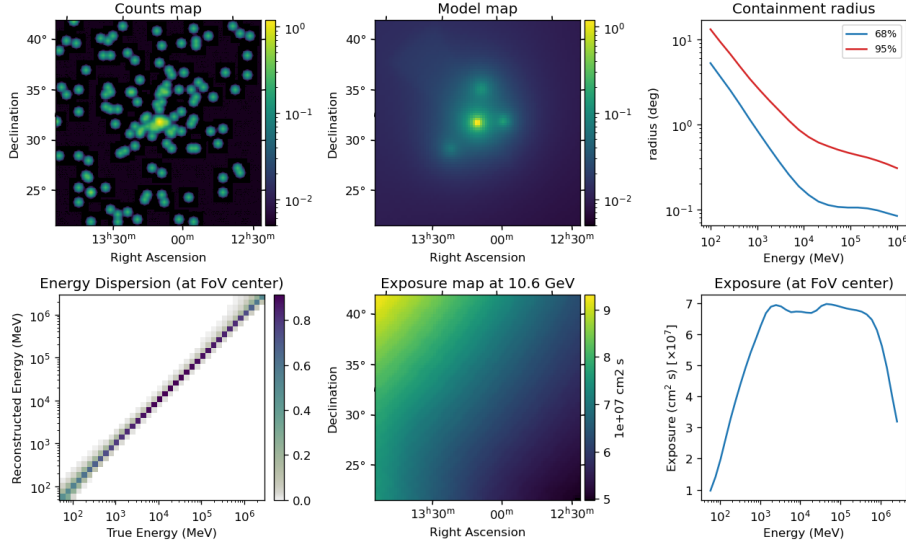


Figure 1: Representation of a 3D MapDataset (in the figure, Fermi-LAT dataset OP 313). From top left to bottom right, a)

1.2 1D Spectral Datasets (X-ray and Cherenkov telescopes, optical spectrographs)

For instruments whose high-level analysis products consist of extracted count-rate spectra with associated responses (e.g. *Swift*-XRT, NuSTAR, and the Cherenkov telescopes in the case of point-like sources), we can forget about the two spatial coordinates and use instead a `SpectrumDatasetOnOff` (Poisson statistics with measured background) or `SpectrumDataset` (Poisson statistics with model background). In X-rays, the standard format for such datasets is known as OGIP. For Cherenkov telescopes, there is still no standardized format available, but both OGIP and initiatives such as GADF provide workable formats to store binned event data. Such datasets consist of:

- Source and background spectra in PHA (counts vs. energy) format extracted from ON and OFF regions.
- Redistribution Matrix Files (RMF) and Auxiliary Response Files (ARF) defining energy dispersion and effective area (or exposure if the effective area is multiplied by the livetime).
- Metadata defining the acceptances for the ON and OFF integration regions, as well as the livetime.

These 1D datasets are significantly lighter than the 3D cubes for *Fermi*-LAT, as they omit the spatial convolution with the PSF or contributions from additional field sources. The corresponding likelihood is fed directly into the forward-folding engine, preserving full Poisson statistics in each energy bin. Special care needs to be given to the reconstructed energy binning for `SpectrumDatasetOnOff`, to ensure that each channel contains a sufficient number of events for Poisson statistics to be applicable.

Liverpool SPRAT, an optical spectrograph working on the Liverpool telescope, also belongs to this category, albeit with some peculiarities worth remarking on. First, the exposure needs to be

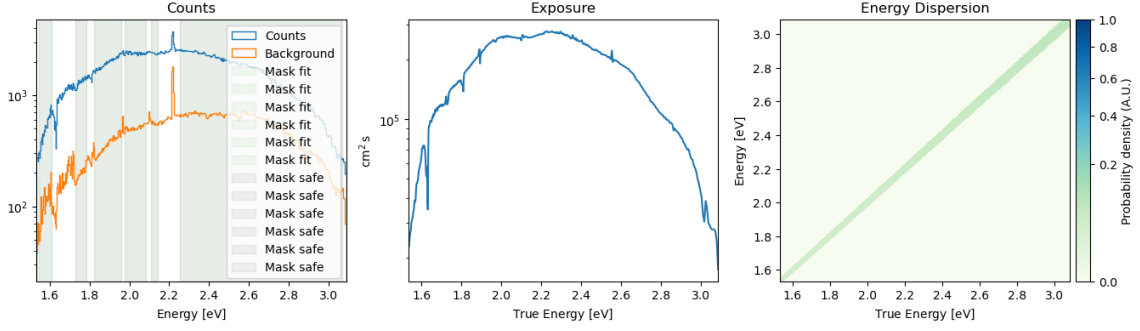


Figure 2: Representation of a 1D SpectrumDatasetOnOff (in the figure, Liverpool SPRAT’s optical spectrum of 4C+27.50). The first panel shows the Source and Background counts spectra, masked to avoid regions dominated by atmospheric lines. Second panel shows the exposure (effective area times livetime). Third panel shows the redistribution matrix (reconstructed energy vs true energy).

estimated, for example, using spectrophotometric standard stars. Second, the redistribution matrix is usually not provided and instead is often approximated by a wavelength $E_{\text{reco}}/E_{\text{true}}$ window, assuming a flat or Gaussian profile with a fixed width.

SPRAT is a low-resolution optical spectrograph on the Liverpool Telescope. Its high-level product is also a 1D spectrum, but with two notable peculiarities: i) The effective area (or exposure) must be derived from observations of spectrophotometric standard stars with known emission spectra. ii) in the absence of an official RMF, we approximate the wavelength redistribution by a Gaussian kernel (or a top-hat window) of fixed width, representing $E_{\text{est}}/E_{\text{true}}$. Despite these approximations, including SPRAT in the joint fit extends the coverage into the optical band with a consistent forward-folding and yields excellent spectral reconstruction with a large potential to constrain the synchrotron component.

1.3 Single-Channel Rate Datasets (UVOT, IO:O photometry)

For single-channel instruments (e.g. *Swift*-UVOT photometric or Liverpool Telescope’s IO:O filter images, we assemble SpectrumDatasetOnOff objects with a single channel, consisting of:

- Measured count rates (or magnitudes converted to flux densities) per broad spectral channel.
- Filter-specific effective areas and zero points, on first approximation estimated using the filter transmission profile and a normalization derived from aperture photometry of non-variable field stars with catalogue photometry measurements.
- A simple Poisson or Gaussian likelihood per channel, depending on count levels.

Although less informative than full spectra with multiple channels, these datasets are easy to build, and seamlessly integrate into the joint likelihood, extending our coverage down to the optical/UV band.

2. Results

2.1 Optical Spectrophotometry of 4C+27.50

We first demonstrate the capabilities of our framework on optical spectrophotometry of the quasar 4C+27.50, using two SPRAT grisms (one more sensitive toward the red, the other more suited for bluer wavelengths) and IO:O photometry (five sloan filters, $u'g'r'i'z'$).

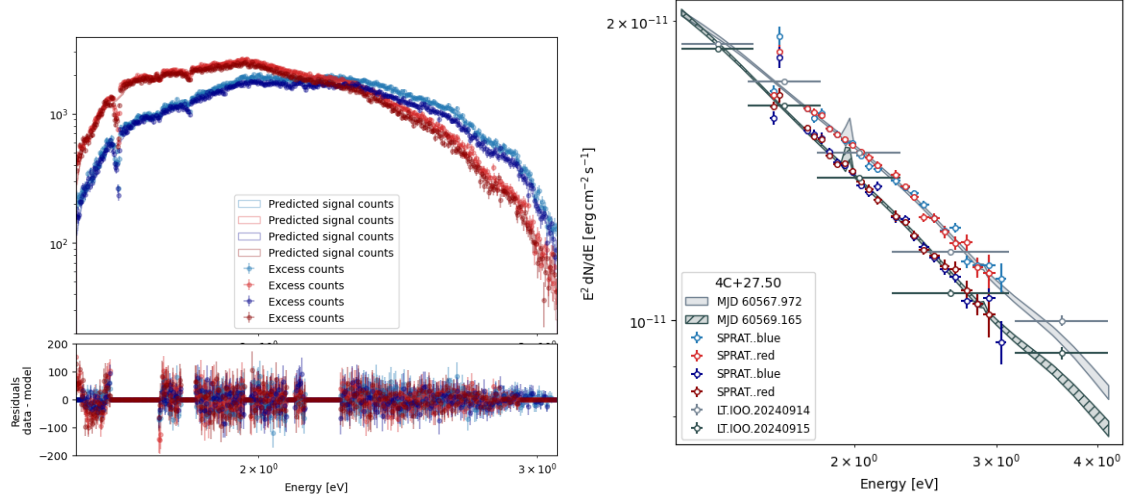


Figure 3: Left: Folded best-fit PWL model, taking into account Galactic extinction, with the instrument response function and residuals for the two SPRAT grisms (red and blue) on two consecutive nights (MJD 60568 and MJD 60569). Each night was fitted independently with a power-law model, the same for the two grisms; error bars are statistical only. **Right:** Joint fit of the two SPRAT grisms (red and blue) and five IO:O filters (Sloan $u'g'r'i'z'$) for nights MJD 60568 and MJD 60569, using a simple PWL spectral model with Galactic extinction. Solid lines show the best-fit power-law; shaded bands are the 68% confidence intervals on the observed flux. Red and Blue flux points are estimation of narrow-band fluxes based on SPRAT. Broad gray flux points are estimated directly using aperture photometry from the IO:O filters.

Both the individual grism residuals (Fig. 3) and the combined SED fits (Fig. ??) exhibit very small scatter and narrow error bands ($\Delta\Gamma \sim 0.01$), underscoring the high precision in the measured spectral indices. This precision directly translates into tight constraints on the synchrotron component and, by extension, the underlying electron energy distribution in the blazar jet.

2.2 Full multi-wavelength forward-folding of OP 313

As a second use case, we apply the unified forward-folding framework to the flaring quasar OP 313, combining

- Optical photometry from Liverpool IO:O (filters $u'g'r'i'z'$),
- UV photometry from *Swift*-UVOT (filters V, B, U and $w1, m2, w2$)
- X-ray spectra from *Swift*-XRT (soft X-rays, 3–10 keV) and NuSTAR (hard X-rays (2–70 keV),
- γ -ray counts cubes from *Fermi*-LAT.

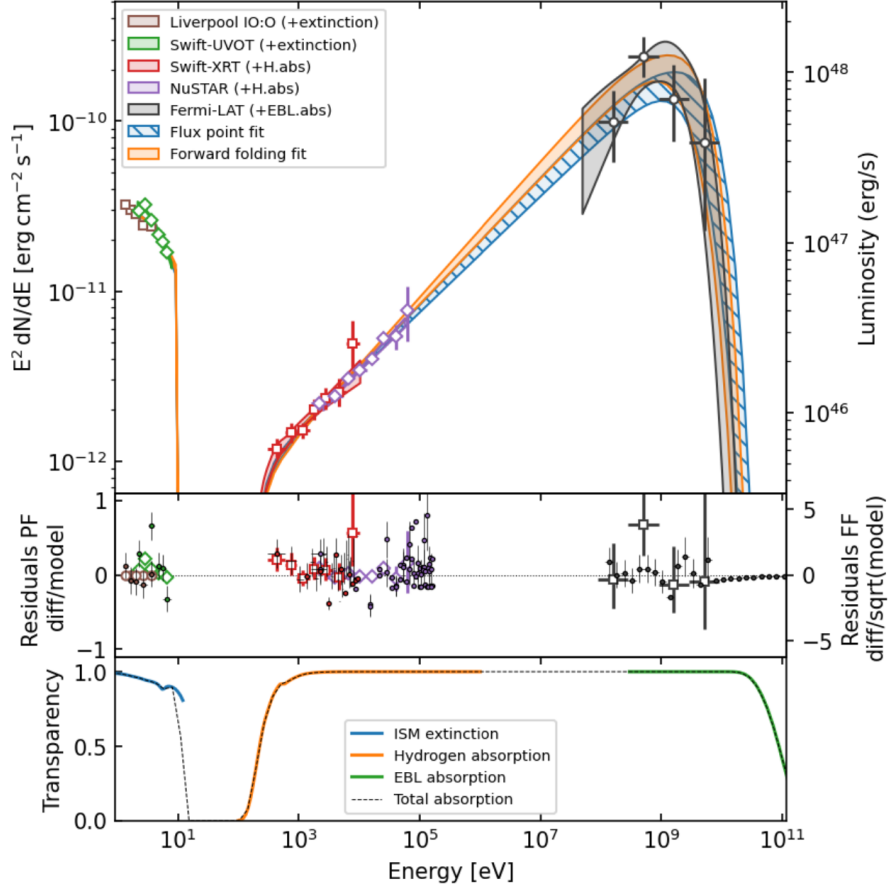


Figure 4: Caption

To illustrate the method, we model the synchrotron and inverse Compton emission from OP 313 as two independent power-law with exponential cut-off models with 3 absorption components: EBL as modelled by aldana-Lopez in the γ -ray band, Xspec’s `tbabs` to model the X-ray absorption in the ISM of our Galaxy from Hydrogen, and `redden` to model the extinction in the optical and UV bands.

The total model is folded with the different instrument response functions for each band (RMF, PSF, exposure or ARF) and the resulting expected counts rates as a function of energy (and spatial coordinates in the case of *Fermi*-LAT) fit to the observed data. This joint fit therefore leverages a single likelihood function across all instruments to reconstruct the broadband spectral energy distribution from optical to GeV energies.

To benchmark the method, we also performed a classic (yet statistically wrong) flux-point fitting across all instruments. Even in OP 313 case, where we basically do not have upper limits and the detection of the source in all bands is sufficiently strong, we notice that: i) the spectral best-fit parameters are similar yet not exactly the same, remarking the importance of using adequate statistics on each dataset; ii) the Forward folding fit manages to constrain the models even in regions where we do not have events coming from the target source (e.g. in the optically-thick EBL

regime, the counts measured from Fermi can still constrain other field sources and diffuse emission components. In the very hard X-rays, > 70 keV, NuSTAR is mostly insensitive to real astrophysical events and most of the counts registered in the detector are instead due to instrumental lines. The data collected with the instrument at such energies can in fact help us estimate the instrumental background from the telescope, in a way similar to the classic overscan techniques used in optical photometry with CCDs); iii) we find slower but slightly more robust convergence in the case of Forward-folding fitting as opposed to the traditional Flux point fitting.

3. Discussion and conclusions

We have presented a brief work extending the `gammapy` analysis package for use in multi-wavelength studies, including optical spectroscopy. The selected quasars, OP 313 and 4c+27.50, are bright quasars at relatively high redshift, ideal to test newly developed methods.

While the limited exposure and scope of these observations preclude strong physical conclusions, the data serve as an excellent benchmark to test new ways of constraining the highly variable non-thermal emission from both targets. In particular, from this work we immediately see the potential of low-resolution spectroscopy (e.g. SPRAT) to strongly constrain the synchrotron component and possible broad emission lines. Such instruments, with very high throughput, allow multiple observations to be performed on a single night and will allow to study in-situ changes in the electron population within the γ -ray emission regions.

These results underscore the importance of coordinated follow-up observations across the electromagnetic spectrum. Future campaigns with increased cadence, broader coverage, or improved sensitivity—particularly combining simultaneous low-resolution spectroscopy and high-energy observations—will be essential to constrain the physical mechanisms at play in these powerful jets.

4. Acknowledgements

M.N.R. acknowledges the support from PID2022-137810NB-C22, funded by MICIN/AEI/10.13039/501100011033 and “ERDF A way of making Europe”, RyC: RYC2021-032991-I, Juan de la Cierva: JDC2022-049705-I, FEDER: Programa Operativo de Crecimiento Inteligente FEDER 2014-2020 (Ref. ESFRI-2017-IAC-12 y ESFRI-2020-01-IAC-12) del Ministerio de Ciencia e Innovación, cofinanciado en un 15% por la Consejería de Economía, Industria, Comercio y Conocimiento del Gobierno de Canarias.

References

- [1] Nieves Rosillo M., Acero F., Otero-Santos J., Vazquez Acosta M., Terrier R., Morcuende D., Arbet-Engels A., 2025, *A&A*, 693, A287. doi:10.1051/0004-6361/202452349
- [2] Acero F., Bernete J., Biederbeck N., Djvuksland J., Donath A., Feijen K., Fröse S., et al., 2024, *zndo*. doi:10.5281/zenodo.10726484
- [3] Atwood W. B., Abdo A. A., Ackermann M., Althouse W., Anderson B., Axelsson M., Baldini L., et al., 2009, *ApJ*, 697, 1071. doi:10.1088/0004-637X/697/2/1071

- [4] Ballet J., Bruel P., Burnett T. H., Lott B., The Fermi-LAT collaboration, 2023, arXiv, arXiv:2307.12546. doi:10.48550/arXiv.2307.12546
- [5] Fermi Science Support Development Team, 2019, ascl.soft. ascl:1905.011
- [6] Harrison F. A., Craig W. W., Christensen F. E., Hailey C. J., Zhang W. W., Boggs S. E., Stern D., et al., 2013, ApJ, 770, 103. doi:10.1088/0004-637X/770/2/103
- [7] Vaughan S., Goad M. R., Beardmore A. P., O'Brien P. T., Osborne J. P., Page K. L., Barthelmy S. D., et al., 2006, ApJ, 638, 920. doi:10.1086/499069
- [8] Roming P. W. A., Kennedy T. E., Mason K. O., Nousek J. A., Ahr L., Bingham R. E., Broos P. S., et al., 2005, SSRv, 120, 95. doi:10.1007/s11214-005-5095-4
- [9] Nigro C., Hassan T., Olivera-Nieto L., 2021, Univ, 7, 374. doi:10.3390/universe7100374
- [10] Steele I. A., Smith R. J., Rees P. C., Baker I. P., Bates S. D., Bode M. F., Bowman M. K., et al., 2004, SPIE, 5489, 679. doi:10.1117/12.551456